NJC

Accepted Manuscript

This is an *Accepted Manuscript*, which has been through the Royal Society of Chemistry peer review process and has been accepted for publication.

Accepted Manuscripts are published online shortly after acceptance, before technical editing, formatting and proof reading. Using this free service, authors can make their results available to the community, in citable form, before we publish the edited article. We will replace this *Accepted Manuscript* with the edited and formatted *Advance Article* as soon as it is available.

You can find more information about *Accepted Manuscripts* in the Information for Authors.

Please note that technical editing may introduce minor changes to the text and/or graphics, which may alter content. The journal's standard Terms & Conditions and the Ethical guidelines still apply. In no event shall the Royal Society of Chemistry be held responsible for any errors or omissions in this *Accepted Manuscript* or any consequences arising from the use of any information it contains.

ROYAL SOCIETY OF CHEMISTRY

www.rsc.org/njc

Revised

Preparation of modified boehmite/PMMA nanocomposites by *in situ* polymerization and assessment of their capability for Cu^{2+} ions removal

Gholamhossein Mohammadnezhad[*] [a], Mohammad Dinari[*] [a], Roozbeh Soltani [a]

[a]*Department of Chemistry, Isfahan University of Technology, Isfahan, 84156-83111, Islamic Republic of Iran*

Abstract A novel organic-inorganic sorbent with good accessible chemically active sites was synthesized and employed for the adsorption of Cu(II) ions from aqueous solutions. Sorbents based on silane modified nano-boehmite and poly(methyl methacrylate) (MBNCs) were prepared by nano-boehmite content of 1, 2 and 3 wt.% via *in situ* polymerization method and their chemical, textural, and structural properties were studied by X-ray diffraction (XRD), thermogravimetric analysis (TGA), transmission electron microscopy (TEM), field-emission scanning electron microscopy (FE-SEM) and FT-IR methods. *In situ* method was applied because of higher percent of polymerization into the nano-boehmite filler matrix. The efficiency of three types of MBNCs for Cu(II) adsorption was examined under the influence of solution pH, contact time, and the batch sorption kinetics for three reaction kinetic models including: pseudo second order, Elovich equation and intra-particle diffusion. The intra particle diffusion model exhibited the two steps occurred during the adsorption process. In

[*]Corresponding authors. Tel.; +98-31-3391-3279; FAX: +98-31-3391-2350.

E-mail address: mohammadnezhad@cc.iut.ac.ir, g_m1358@yahoo.com (G. Mohammadnezhad).

E-mail address: dinari@cc.iut.ac.ir; mdinary@gmail.com (M. Dinari).

New Journal of Chemistry Accepted Manuscript

addition, MBNC 3% exhibited a highly effective removal capability for Cu(II) ions in comparison to the other two types.

Keywords; Nano-boehmite, Poly(methyl methacrylate); In situ polymerization; Transmission electron microscopy (TEM); Adsorption

1. Introduction

Nanofillers including carbon nanotubes (single or multiwall) (CNTs), layered double hydroxide's (LDHs), porous carbon and silica materials, nanoclays, metal oxides, and so on, offering the promise of a variety of new composites, coatings, adhesives, and sealant materials with unique properties.[1] In recent years, research and development on nano-size and porous materials as fillers has attracted increasing interest in many applications due to its excellent physicochemical properties as well as chemical resistance, large surface areas, uniform framework structures and readily controlled diameters.[2] Such properties make them as an excellent reinforcing agent for the fabrication of novel structured polymer nanocomposite (NC) materials in comparison to the virgin materials. Industries are interested in such NCs because they offer promising future in many widespread applications.[3,4] It has been shown that one of the best methods to improve the performance of polymers is dispersion of inorganic nanofillers into polymer matrices. Consequently, the thermal and mechanical properties,[5] electrical conductivity[6] and others properties of such NCs have been greatly improved.[7-9]

Alumina (Al_2O_3) as a metal oxide, exists in large amounts in the earth's crust and is one of the most cost effective and widely used material in the industrial world due to its excellent properties including heat resistance, nontoxic, corrosion resistance, and electric insulation.[10,11] With an excellent combination of properties and an attractive price, it is no surprise that alumina derivatives have attracted considerable industrial and scientific interest

New Journal of Chemistry Accepted Manuscript

in very wide range of applications. Boehmite is a mineral of partially dehydrated aluminum hydroxide (γ-AlOOH) containing hydroxyl groups attached to its surface and is also a crucial precursor for preparation of γ-Al_2O_3. It always crystallizes in the orthorhombic dipyramidal system (Al is surrounded by six O-atoms in a distorted AlO_6 octahedron) with microcrystals or nanocrystals and also can have different morphologies.[10] The crystal structure of alumina have a good thermal stability.[11] Up to now, various morphologies of boehmite nanostructures have fabricated such as hollow microspheres,[12] nanosheets,[13] nanofibers,[14] nanowires,[15] nanorods and nanotubes.[16,17] The acidic and basic centers on the surface of boehmite make it very useful for many applications because of functionalizable surface in nanometric scale. In addition, boehmite has a good porosity, transparency, chemical resistance, high hardness, and very large surface area. These remarkable characteristics of nano-boehmite (γ-AlOOH) and its oxide derivatives such as α-Al_2O_3 and γ-Al_2O_3 have been investigated widely because they can be used in advanced catalysts,[18,19] flame retardants,[20] toxic materials, heavy metal adsorbents,[21-23] support for biomolecules and drug delivery,[24,25] and precursor in NCs.[26,27]

Poly(methyl methacrylate) (PMMA) is one of the most widely used polymers in industries which find applications in home products, medical and health industries, electronic and energy, architecture and construction and more. PMMA is a thermoplastic polymer, transparent and rigid material with low water adsorption that can be easily synthesized by several different techniques.[28] Recently, numerous studies on PMMA have been undertaken and considerable efforts have been reported towards the preparation of NCs of PMMA having different properties. In order to upgrade the properties of PMMA, composites have been recommended by dispersing the nanoscale fillers in polymer matrices. The incorporation of these materials into PMMA matrix can be achieved by four general methods, template synthesis, *in situ* synthesis, melt intercalation or melt blending techniques and intercalation of polymer from solution.[29] Template synthesis involves the synthesis of inorganic material in

New Journal of Chemistry Accepted Manuscript

the presence of polymer matrix. In melt blending synthesis, the high molecular weight polymer melts at high temperature under pressure. High temperature for mixing of organic and inorganic components may lead to the thermal degradation of the modified filler and polymer. Also, degradation can alter filler matrix and its properties.[29-31] In intercalation of polymer from solution, both organically modified nanofiller and polymer is dispersed in a common solvent. The polymer then adsorbs onto the porous structure and delaminated sheets follow by the evaporation of the solvent. When the solvent is evaporated, polymer chains are trapped between the sheets and an ordered multilayer structure is generally formed using this approach. In this method only water-soluble polymers, like poly (vinyl alcohol), poly (acrylic acid), poly (ethylene oxide) and etc., are mostly used.[29,32] In the *in situ* synthesis approach, the nanofillers are swollen/dispersed in monomer solutions. After swelling, the polymerization of the monomer initiate by addition of the initiator. As monomers are present in and out of the filler, polymerization initiates in and out of the filler interlayers.[29,33] Thus, for the control of intragallery and extragallery polymerization reactions, modification of the monomer with the organic moiety is usually used. The modified fillers have specific interaction with the matrix polymer and these interactions are responsible for the ability of the fillers to well dispersion and inhibition of filler aggregation into polymer matrix.[34,35] To date *in situ* polymerization has produced the best dispersed systems for NCs.[35]

Industrial activities including metal painting, plating, battery manufacturing, mining operation, fertilizer and leather tanning, discharging heavy metals in aqueous waste streams and environment, are responsible to generate various adverse health effects to living organisms and human`s health specially.[36] Unlike organic contaminants, inorganic materials including heavy metals and their compounds are not biodegradable and do not break down into less harmful species gradually. Also, heavy metals generally tend to accumulate in living organisms over time. Accordingly, one of the most important issues becomes a critical

New Journal of Chemistry Accepted Manuscript

worldwide concern, is the inadequate access to the safe water. So, it is important to adsorb and remove these harmful materials from the wastewater before releasing of them into the environment. In recent years, many methods have reported to remove heavy metal ions include membrane filtration,[37] ion exchange,[38] adsorption,[35,39] solvent extraction[40] and chemical precipitation-coagulation.[41] Among all of the methods, adsorption has gained special interest as a more effective alternative method. In spite of the advantages mentioned, adsorption method is a promising approach for the removal of heavy metal at low concentration (1-20 mg/L).[41]

In this paper, we report the synthesis and characterization of NC materials based on modified boehmite/PMMA nanocomposites (MBNCs). Methyl methacrylate (MMA) immobilization onto the silane modified mesoporous boehmite structure and subsequent addition of initiator and polymerization resulted in the formation of high polymer content into the nanofiller. The obtained MBNCs exhibited good potential for adsorption of Cu(II) ions in aqueous solution due to the presence of many chemically active sites of organic-inorganic sorbent in it. The factor affecting the adsorption process of Cu(II) including pH and contact time and also its adsorption behavior with three adsorption kinetic models were studied.

2. Experimental

2.1. Materials

3-Mercaptopropyl-trimethoxysilane, copper(II) nitrate trihydrate [$Cu(NO_3)_2.3H_2O$], 2-propanol, methylmethacrylate (MMA), benzoyl peroxide (BP), and acetic acid were purchased from Merck Chemical Co. and used without further purification. Nano-boehmite was synthesized based on the modified procedure.[42]

2.2. Instruments

New Journal of Chemistry Accepted Manuscript

Crystalline structure of samples were examined by a Philips Xpert MPD diffractometer equipped with a Cu Kα anode (λ = 1.540 Å) for 2θ, in the range of 5-80°. FT-IR spectra were recorded with a Jasco-680 (Japan) spectrometer from 400 to 4000 cm^{-1}, using KBr pellet by making 60 scans at 4 cm^{-1} resolution. Thermogravimetric analysis (TGA) of the samples were carried out in a nitrogen atmosphere by heating rate of 10 °C/min from room temperature to 800 °C using the STA503 TA instrument. The morphology of the nanostructure materials was examined by FE-SEM (HITACHI, S-4160) and TEM (Philips CM 120, Netherlands). The sono-chemichal reactions were carried out on a MISONIX ultrasonic liquid processor, XL-2000 SERIES (Raleigh, North Carolina, USA). Ultrasound was a wave of frequency 2.25×10^4 Hz and power of 100 W. The concentrations of the metal ions in the solution were measured by use of flame atomic absorption spectrophotometer (Perkin-Elmer 2380-Waltham).

2.3. Modification of boehmite with 3-mercaptopropyl-trimethoxysilane

The surface of the boehmite nanoparticles was functionalized with 3-mercaptopropyl-trimethoxysilane by the following procedure: 0.30 g of boehmite and 20wt.% of silane coupling agent (0.06 g) were added into ethanol and subjected to ultrasonic irradiation for 1 h. Then the solution was refluxed for 6 h and subjected to ultrasonic irradiation for subsequent 2 h. Finally, the obtained suspension was filtered, washed with a large amount of ethanol to remove unreacted silane coupling agent and dried at 60 ^oC for 24 h. The mercapto-modified nano-boehmite sample was called MB.

2.4. In-situ synthesis of modified boehmite/PMMA nanocomposites (MBNCs)

NC materials with boehmite contents of 1, 2, and 3 wt.% were synthesized using an *in situ* approach. In this procedure, different amounts of MB (0.02, 0.04 and 0.06 g) were added to 6 mL of dry toluene and sonicated in an ultrasonic bath for 1 h. Definite amounts of MMA

New Journal of Chemistry Accepted Manuscript

were added to the solution of the MB. The monomer/boehmite mixture was mixed at room temperature under stirring to obtain a stable suspension and sonicated for 1 h before addition of the initiator. The benzoyl peroxide (BP), the initiator (1 wt.%), was added into the suspension and reaction temperature was adjusted at 80-90 °C. Then the mixture was refluxed for 6 h. The polymerization was carried out under isothermal conditions. The sample solution was then poured into a clean plastic petri dish, and the solvent was evaporated under a nitrogen atmosphere. Further vacuum and heat treatment (60 ^{o}C) led to dry and glassy film consisting of PMMA and MB. Using the above *in situ* synthetic approach, we synthesized three types of MBNCs to adsorb Cu^{2+} ions from the aqueous solution.

2.5. Adsorption studies: copper removal over MBNCs

Aqueous solutions of Cu(II) were prepared by dissolving the analytical grade $Cu(NO_3)_2.3H_2O$ (>99.0% purity) in deionized water. For each experiment, a volume of 10 mL of aqueous solutions, containing Cu(II) at concentration of 10 mg/L, was taken in 100 mL capped polypropylene bottles. Afterwards, 10 mg of adsorbent (MBNCs) was introduced. The resulting suspensions were agitated on a Shaker at 150 rpm at room temperature (25 ºC) and the contact time was varied from 15 to 240 min. At the end of the predetermined time intervals, the adsorbent was separated by centrifugation (6000 rpm, 10 min) and filtered through a 0.45 μm filter membrane. The adsorption capacity of adsorbents was calculated from the difference between the initial and the final concentrations of Cu(II) ions. Flame atomic absorption spectrometer was used for determination of the amount of Cu(II) by calibration curve.

3. Results and discussion

3.1. Preparation of MBNCs

New Journal of Chemistry Accepted Manuscript

The overall strategy applied for the preparation of MBNCs by the *in situ* synthesis approach was shown in Scheme 1. One of the most remarkable features of boehmite (AlOOH) is its abundant hydroxyl active groups on the surface. Surface modification of such nanofillers facilitates its interactions with desired organic molecules. In fact, surface modification provided a high active accessible surface area for better interaction with different functional groups. MMA, as a monomer, can be easily interacting with the modified boehmite. So, before the start of the polymerization in the presence of initiator, monomers can be distributed in the filler matrix. Accordingly, the polymerization process can be take place after addition of initiator into the system. -OH and -SH groups on the surface of modified boehmite and carbonyl groups of polymer moiety may interact by hydrogen bonding during polymerization procedure and lead to the formation of polymer chains through the modified filler. Hence, the advantage of this polymerization method compared to other methods is the higher percent of polymerization into the filler matrix.

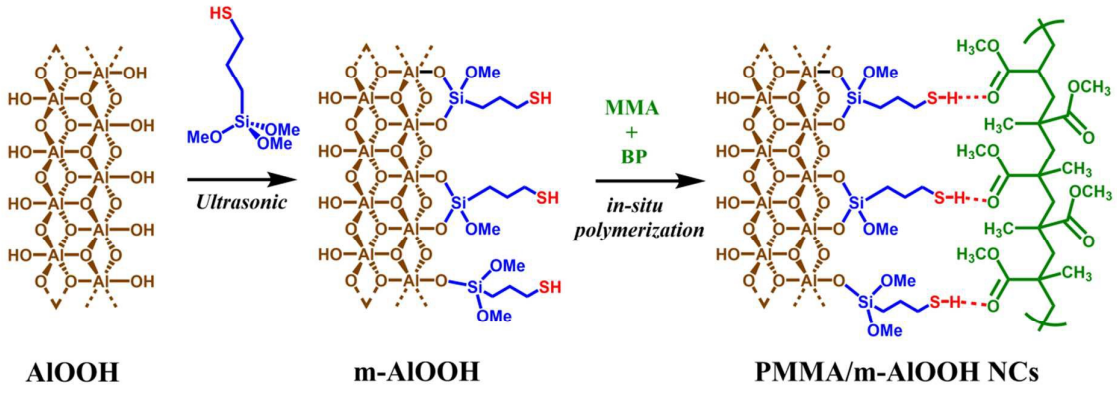

Scheme 1. Surface modification of nano-boehmite and preparation of MB/PMMA hybrid materials by *in situ* polymerization.

3.2. Characterization studies

Fig. 1 represents the FT-IR spectra of the pristine boehmite and MB. In the FT-IR spectrum of pure boehmite, all the absorption characteristic peaks at 3444, 1629, 1069, 878, 621, and 483 cm^{-1} are present.[13] FT-IR spectrum of the pure boehmite had characteristic bands at

New Journal of Chemistry Accepted Manuscript

around 1069 cm^{-1} which originates from the Al-O bonds vibrations, a weak band at 1629 cm^{-1} which is assigned to the bending mode of absorbed water, 621 cm^{-1} is attributed to vibration of AlO_6, and a strong broad band around 3444 cm^{-1} assigned to stretching vibration of OH group present both at the surface and in the bulk of the solid (Fig. 1a). In the FT-IR spectrum of the modified boehmite, a characteristic absorption peak at 1068 cm^{-1} is due to the vibration of Si-O bond. Another peak appeared at 781 cm^{-1} attributed to the Si-OH group. The peak at 2929 cm^{-1} corresponded to the CH bonds (Fig. 1b). Thus, the above characteristic peaks indicated the reaction of silane coupling agent with boehmite.

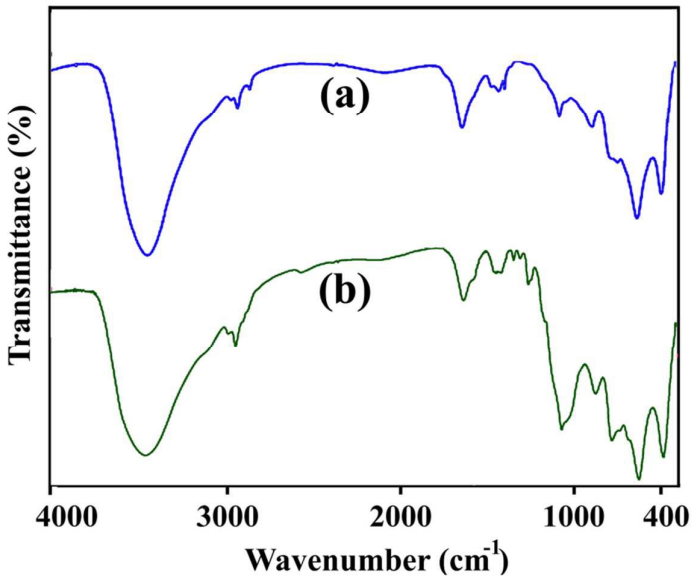

Fig. 1. FT-IR spectra of the pure boehmite (a) and modified boehmite (b).

Fig. 2 provides the FT-IR spectra of pure PMMA and NCs samples containing 1%, 2% and 3% (w/w) of MB. The band at 1731 cm^{-1} is attributed to the vibration of the C=O, which is typical band of PMMA (Fig. 2a). Two bands at 1486 and 1450 cm^{-1} originating from the O–CH_3 bending vibrations and a strong peak at 1148 cm^{-1} associated with the C-O stretching mode. Also, the two absorption peaks around 2998 $cm^{-1}$and 2952 cm^{-1} assigned to the C-H asymmetric stretching of CH_3 and CH_2, respectively. The vibrational band at 2845 cm^{-1} was

New Journal of Chemistry Accepted Manuscript

owing to the C-H symmetric stretching in CH_3 also is observed. The vibrations due to the deformation modes of CH_3 groups appeared at 1272, 1243 and 1194 cm^{-1} (Fig. 2a).[43] In PMMA/MBNCs, the carbonyl absorption remains at 1731 cm^{-1}, and O–CH_3 bending bands (1450, 1486 cm^{-1}), C–O stretching band (1148 cm^{-1}), the C–H stretching vibration (2952, 2998 cm^{-1}), and C–H asymmetric stretching are similar to those observed for pure PMMA (Fig. 2b-2d). Also the peak of Al-O stretching at 1069 cm^{-1} is hidden within the 1148 cm^{-1} peak of the C-O vibration. A broad band around 3500 cm^{-1} in three types of NCs assigned to stretching vibrations of OH groups of the MB.

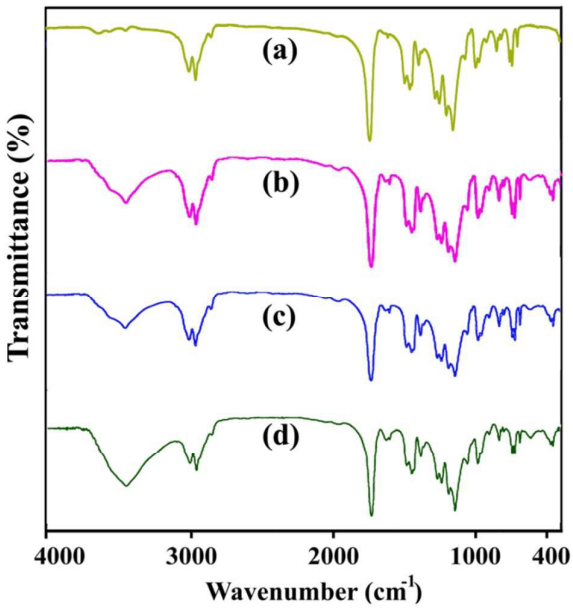

Fig. 2. FT-IR spectra of the neat PMMA (a) and NCs of PMMA with 1, 2, and 3 wt.% of modified boehmite (b-d, respectively).

The XRD patterns of the nano-boehmite, MBNCs 2wt.% and 3wt.% are shown in Fig. 3. As shown in this Fig. 3a, XRD analysis confirmed that boehmite was formed and the XRD pattern of the boehmite having nano-sized particles showed typical peaks of boehmite at around 2θ = 28°,49°,and 65°. These peaks were smaller in height but wider in width than those of crystalline boehmite which means that the nano-boehmite particles are formed. For

New Journal of Chemistry Accepted Manuscript

preparation of MBNCs, 2wt.% or 3wt.% of nano-boehmite were used and the diffraction peaks intensity were actually affected by the introduction of the large content of organic substrate. As a result, the XRD patterns of MBNCs did not show sharp diffraction peaks as shown in Fig. 3.

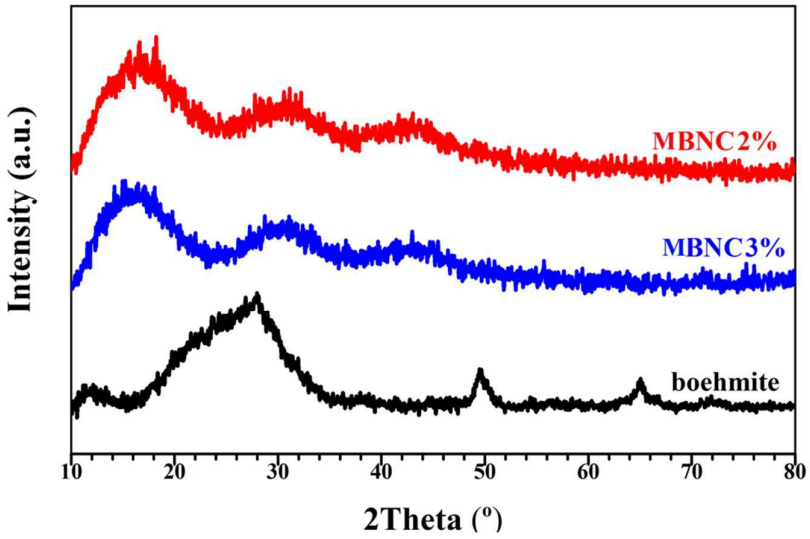

Fig. 3. XRD patterns of the boehmite and NCs of PMMA.

Figs. 4a-4d showed the morphological information of the nano-boehmite and MB, respectively. As shown in these Figs., pristine boehmite have flake like morphologies and after modification process, the surface morphology of the MBs were changed to spherical shapes. To investigate the dispersion of the MB within the polymer matrix for MB contents of 1, 2 and 3 wt%, the morphology of the hybrid materials were examined by FE-SEM technique (Fig. 5). In comparison to pristine PMMA (Figs. 4e and 4f) which showed a smooth surface, the fracture surface of the MBNCs had become rougher that of the pure polymer and particles were observable, suggesting that MB distribution into the PMMA matrix. For the 1, 2, and 3wt% MBNCs, the filler has spherical morphology and is seemingly homogeneous due to the good adhesion to the organic polymer (Fig. 5).

New Journal of Chemistry Accepted Manuscript

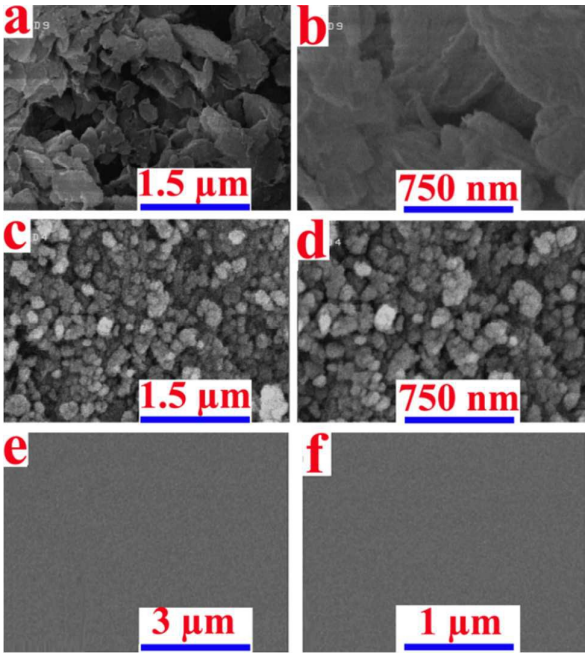

Fig. 4. FE-SEM images of boehmite (a,b), m-boehmite (c,d), and pure PMMA (e,f).

The morphology of nano-boehmite and the distribution of its modified particles in the PMMA matrix were also studied by TEM technique. The typical TEM images clearly show that the pristine nano-boehmite has a fibrous shaped structure with an average length of 30 nm (Figs. 6a and 6b). After polymerization of MMA in the presence of 2wt% of MB and subsequent preparation processes, the morphology of the MBNCs were changed to nanosized spheroidal particles having diameter with less than 10 nm (Figs. 6c and 6d).

New Journal of Chemistry Accepted Manuscript

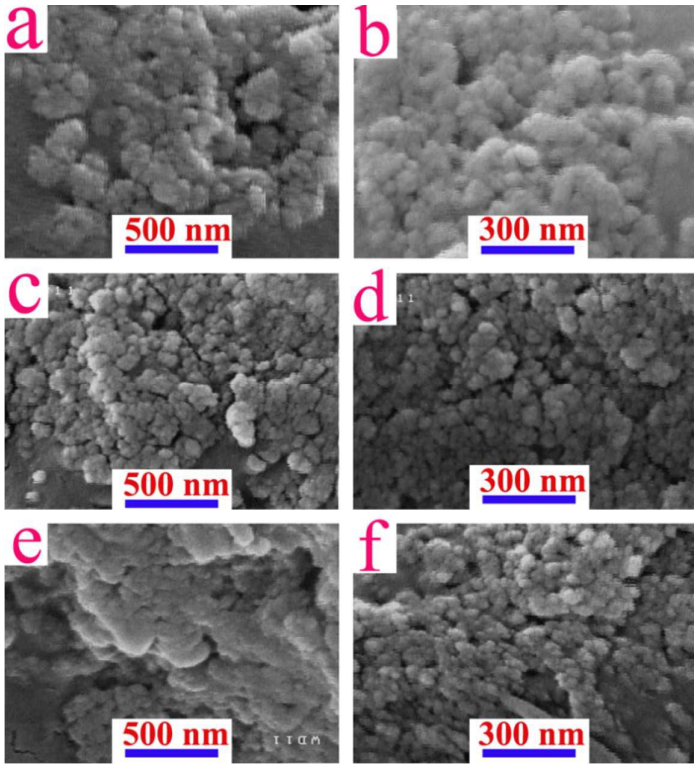

Fig. 5. FE-SEM images of NCs of PMMA with 1 (a,b), 2 (c,d) and 3 wt.% (e,f) of m-boehmite.

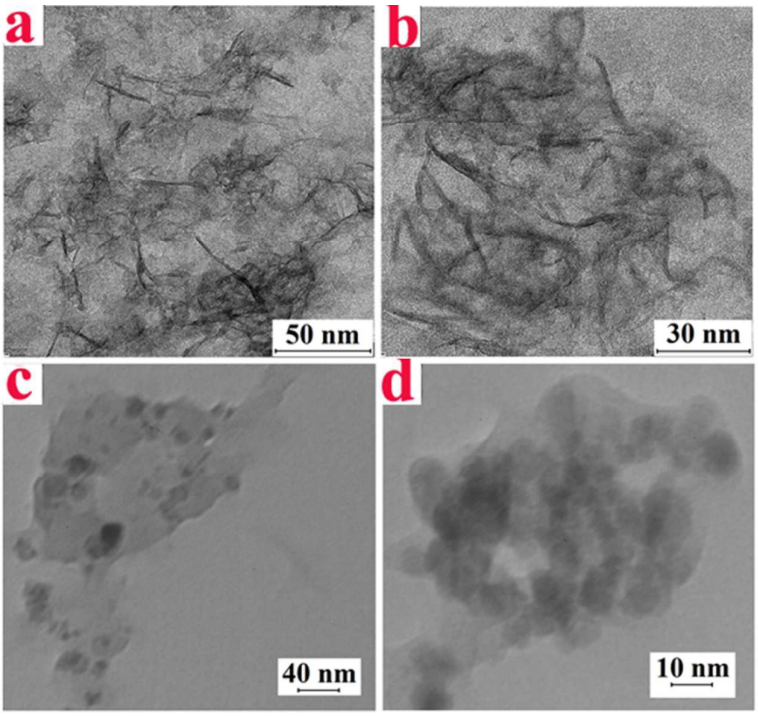

Fig. 6. TEM images of pure boehmite (a, b) and MBNC with 2 wt.% of m-boehmite (c, d).

New Journal of Chemistry Accepted Manuscript

The thermal stability of the synthesized materials based on PMMA with different amount of MB (1, 2, and 3%) was evaluated by TGA technique under a N_2 flow. Fig. 7 shows the TGA curves of pure PMMA and NC of PMMA with 1, 2 and 3wt % of MB. The TGA data showing the temperature at which 5% degradation occurs, T_5, the temperature at which 10% degradation occurs, T_{10}, and the amount of material which is not volatile at 800 ^oC, char; are shown in Table 1. The mass loss behavior of PMMA/MB NCs could be explained in comparison with neat PMMA. The 5% and 10% mass loss temperatures of the NCs were higher than those of the pristine PMMA and according to the obtained results, the maximum degradation temperature of the NCs has been shifted to higher region as the amount of MB is increased. By adding only 2 wt % of modified MB, the initial degradation temperature of PMMA increases by 90 ^oC. This data shows that the incorporation of MB hybrids increase the thermal stability of the resulting NCs. Char residues (CR) at 800 ºC of the composites with different modified boehimite content are 4-9% which they are higher than that of pure PMMA (2%). It appears from these data that the AlOOH particles enhance the thermal stability of PMMA. These TGA data illustrated an improvement in the thermal stability of PMMA by the presence of MB. This improvement of thermal stability of PMMA in the presence of MB can be explained by:[26,44]

i. Polymer chains mobility restrictions. Certainly, it is well known that the filler surface has a marked effect on molecular mobility in a filled polymer.

ii. Radical trapping effect of these mineral fillers.

iii. The adsorption of polymer on filler surfaces via the methoxycarbonyl groups.

New Journal of Chemistry Accepted Manuscript

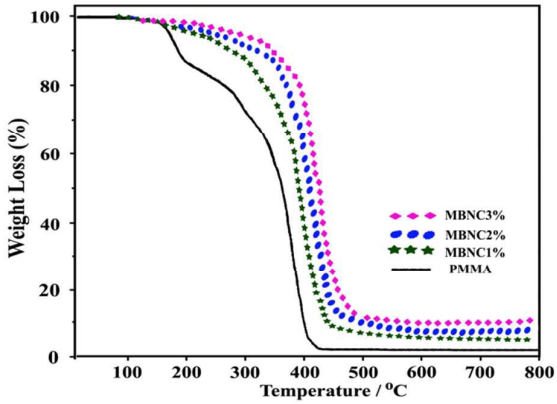

Fig. 7. TGA thermograms of the pure PMMA and different NCs.

Table 1. TGA data of neat PMMA and different NCs of PMMA and modified boehimite

Samples	T_5 (°C)[a]	T_{10} (°C)[a]	Char yield (%)[b]
PMMA	178	194	2
MBNC1%	233	288	4
MBNC2%	267	321	7
MBNC3%	293	356	9

[a] Temperature at which 5% and 10% weight loss was recorded by TGA at heating rate of 10 °C/min under a nitrogen atmosphere. [b] Weight percentage of material left undecomposed after TGA analysis at a temperature of 800 °C under a nitrogen atmosphere.

3.3. Adsorption studies: copper removal over MBNCs

In this study, we have chosen Cu(II) for the adsorption experiments due to serious problems that Cu(II) can be caused in living organisms. The accumulation of copper (II) in the human body in a high unallowable amount can cause eminent health problems, such as heart, brain, skin, kidney, and pancreas damages.[45]

New Journal of Chemistry Accepted Manuscript

The removal of Cu(II) using three types of MBNCs was investigated and the influence of two important parameters including pH and contact time were monitored (Scheme 2). The impact of these two parameters on the adsorption processes is shown in the Fig. 8. The removal efficiency was calculated as follow:

$$\%\, Removal = \frac{C_i - C_e}{Ci} \times 100 \quad (1)$$

Where C_i and C_e are the initial and final (equilibrium) concentrations of the Cu(II) ions in aqueous solution (mg L^{-1}).

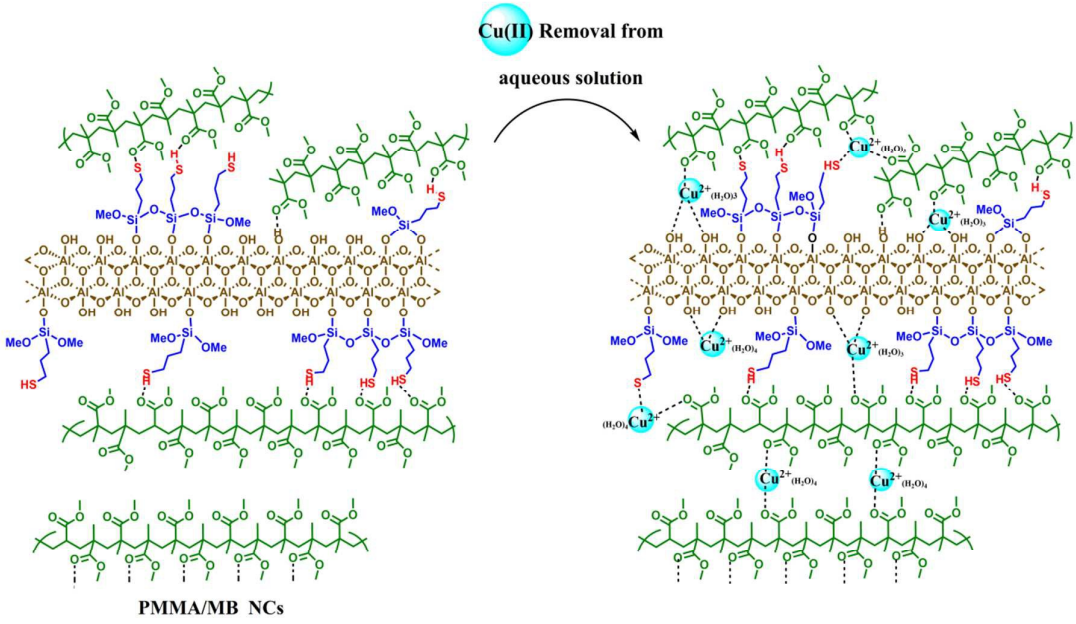

Scheme 2. Schematic representation for removal of Cu(II) by MB/PMMA hybrids.

3.3.1. Effect of pH on the adsorption

The effect of pH on the adsorption of copper ions is shown in Fig 8a. It was evident that the pH media played an essential role to the adsorption capacity of adsorbents for heavy metals ions in aqueous media due to its effect on the surface charge of the adsorbent and solution chemistry of heavy metals.[46] To determine optimum pH for the maximum removal

New Journal of Chemistry Accepted Manuscript

of Cu(II), the equilibrium adsorption of copper was measured at different pH levels (from 1.5 to 6.5) by setting the initial Cu(II) concentrations at 10 ppm. The removal percentages of copper at pH=2.0 were below 10% for all three types of MBNCs. The lower adsorption capacity can be attributed to the competition of Cu(II) with H^+. In other words, an excess of H^+ ions in solution tended to occupy the attainable active area on the MBNCs and competed efficiently with copper ions due to electrostatic forces at low pHs. Accordingly, fewer accessible binding sites for Cu(II) lead to less adsorption of copper ions in the presence of excess H^+ ions. It was found that the removal efficiency of Cu(II) ions on tree type of MBNCs increased rapidly with the increase of pH from 2.0 to 4.0 and then it does not change greatly with further increase of pH from 4.0 to 6.5. The maximum uptakes is obtained at pH=4.0, about 95.24%, 92.02%, 80.73% for MBNCs 3%, 2% and 1%, respectively. Therefore, pH=4.0 was selected as an optimum pH. The increasing adsorption capacity might be ascribed to the conversion of surface -OH groups to $-O^-$, formation of surface negative charge, and consequently electrostatic interactions between the cationic form of copper and active surface functional groups such as carbonyl, mercapto and hydroxyl.

3.3.2. Effect of the contact time

The effect of the contact time was another key factor which was determined. Fig. 8b exhibited that the adsorption equilibriums were achieved when the contact time reaches 120, 120 and 150 min for the MBNCs 3%, 2% and 1%, respectively and leveled off gradually until the Cu(II) adsorption showed no considerable increasing and removal has finally reached equilibrium. Also, the obtained results revealed that the adsorption process possess an approximately fast kinetics due to the highly accessible active sites on the surface of MBNCs and the well dispersion of MBNCs in aqueous phase. Decreasing in removal process could be explained by occupying of active coordination sites such as -OH, SH and carbonyl groups.

New Journal of Chemistry Accepted Manuscript

Within exposure time of 240 min, the adsorbed Cu(II) percentage by entrapped MBNCs reached to 94.29 %, 92.24 % and 81.02% for MBNCs 3%, 2% and 1%, respectively.

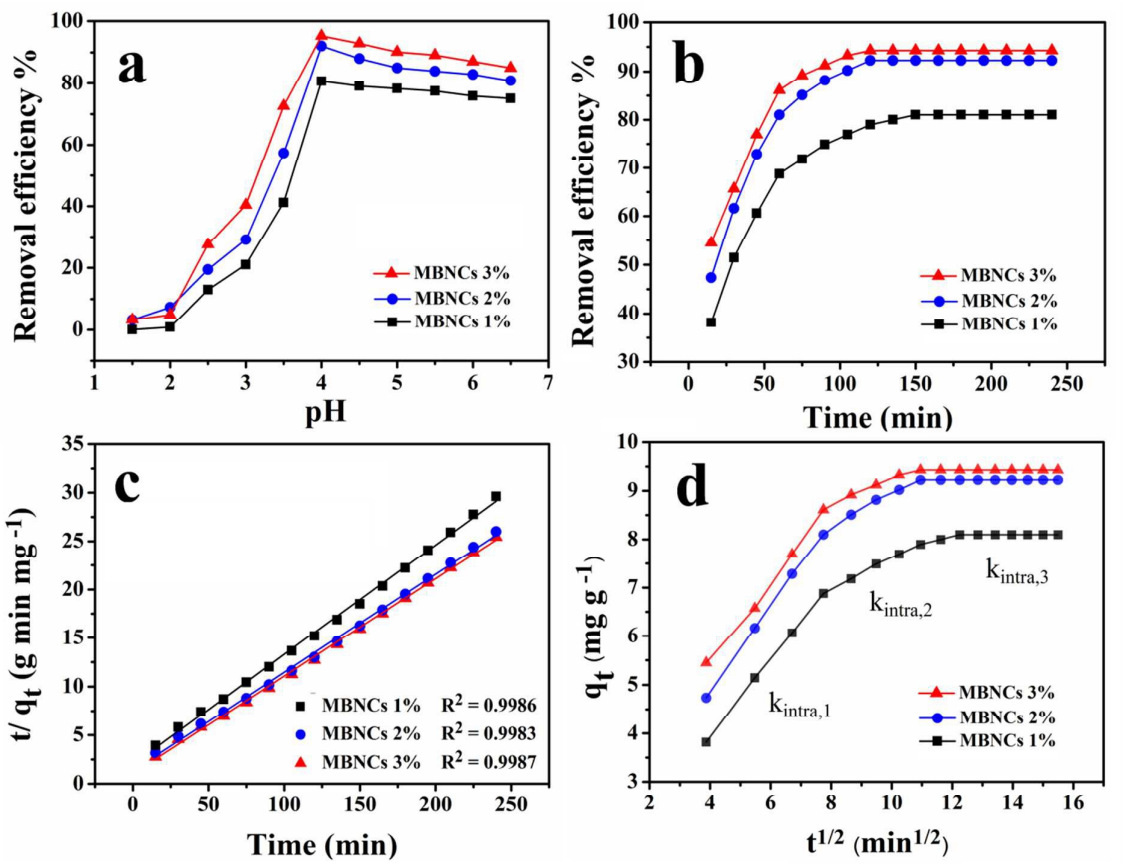

Fig. 8. Effect of pH for Cu(II) adsorption by the MBNCs (a), and the effect of contact time for the optimum Cu(II) ions adsorption (b) when the MBNCs amount was 10 mg, optimum pH=4.0, and the Cu(II) ions concentration was 10.0 mg/L (b), Pseudo-second-order kinetics plots for the adsorption of Cu (II) (c), and the intra-particle diffusion rate constants of Cu(II) adsorption by MBNCs (d).

3.3.3 The adsorption kinetic studies

The kinetic study is useful to find an appropriate mechanism of adsorption kinetic models and determine the efficiency of the adsorption which is very essential to designing and modeling of the adsorption process. The amount of Cu(II) ions at any time t (q_t, $mg\ g^{-1}$) and retained in the sorbent phase at equilibrium (q_e, $mg\ g^{-1}$) was calculated by:

New Journal of Chemistry Accepted Manuscript

$$q_e = \frac{(C_i - C_e)V}{m} \quad (2)$$

$$q_t = \frac{(C_i - C_t)V}{m} \quad (3)$$

Where C_t $(mg\ L^{-1})$ is the Cu(II) concentrations at time t, V(L) is the aqueous solution volume, and m (g) is the mass of MBNCs. In addition, the distribution coefficient (K_d)[44] of Cu(II) ions, indicating sorption performance of MBNCs, was calculated according to equation 4:

$$K_d = \left[\frac{C_i - C_e}{C_e}\right] \times (V/m) \quad (4)$$

Where V is the solution volume (mL). Higher K_d values representing more effective sorbents for the removal of Cu(II).[47]As shown in Fig. 9, MBNC 3% has a higher amount of K_d than those of the MBNC 1% and MBNC 2%, expressing that MBNC 3% is a better adsorbent for removal Cu(II).

To investigate changes in sorption of metal ions with time and the adsorption kinetics of Cu(II), three kinetic models, pseudo-second-order,[48] Elovich,[49] and intra-particle diffusion model,[50] were used to simulate the experimental data. In order to investigate the accuracy of these kinetic models in predicting the Cu(II) ions' adsorption behavior, the correlation coefficient (R^2) of each model was calculated.

The pseudo-second-order expression is given as:

$$\frac{t}{q_t} = \frac{1}{k_{ad} q_e^2} + \frac{1}{q_e} t \quad (5)$$

Where k_{ad}, is the rate constant of pseudo second order equation $(g\ mg^{-1} min^{-1})$. The initial adsorption rate: $h = k_{ad} q_e^2 (mg\ g^{-1} min^{-1})$ and q_e $(q_{e,cal})$ and k_{ad} can be calculated from the plots of t/q_t versus t (Fig. 8c).

Elivich equation is expressed in the following form:

$$q_t = \frac{\ln(h\beta)}{\beta} + \frac{\ln(t)}{\beta} \quad (6)$$

New Journal of Chemistry Accepted Manuscript

Where β is the desorption constant ($mgg^{-1}min^{-1}$). Furthermore, the intraparticle diffusion model can be represented by Weber and Morris equation:

$$q_t = k_{intra}(t)^{1/2} + C \qquad (7)$$

Where k_{intra} is the intra-particle diffusion rate constant ($mg\ g^{-1}min^{-1/2}$) which can be calculated from the slope between q_t vs. $t^{0.5}$ and C is a constant. The plotting of q_t vs. $t^{0.5}$ was shown in Fig. 8d. The intra-particle diffusion rate constants (k_{intra}) were calculated and listed in Table 3. According to this model, when the plots passes through the origin (C=0) the intra-particle diffusion plays a role in the rate controlling stage. Whereas, if the line does not pass through the origin, it can be explain that some degree of boundary layer control is present. In this case, the other kinetic models may control the rate of adsorption and intra-particle diffusion is not the only rate-limiting stage.[51] The correlation coefficient (R^2) values of the three kinetic models and other related kinetic parameters were calculated and listed in Table 3. Due to the proximity of R^2 values of the investigated three kinetic models, pseudo-second-order model could be consider as a suitable model for interpretation of adsorption mechanism. Also, the $q_{e,cal}$ values using the pseudo-second order kinetic model for three types of MBNCs agreed well with the experimental values ($q_{e,exp}$). Suggesting the process controlled by chemical adsorption which might involve the valency forces through sharing or exchange of electrons between Cu(II) ions and adsorbents.[52] Additionally, the intra-particle diffusion model could indicate a good picture of adsorption process. According to Table 3, it is obvious that the order of adsorption rates is $k_{intra,1} > k_{intra,2} > k_{intra,3}$ for three types of MBNCs. At the beginning, Cu(II) was adsorbed by the exterior surface of MBNCs, and the first linear region was the instantaneous diffusion period (slope $k_{intra,1}$) within the first 60 min), during which nearly 86%, 81% and 67% of Cu(II) were adsorbed by exterior surface (film diffusion) of MBNCs 3%, 2% and 1%, respectively. When adsorption on exterior surface reached to saturation, second linear stage begins. The copper ions entered into the

New Journal of Chemistry Accepted Manuscript

pores of boehmite in the MBNCs texture through intra-particle diffusion. With Cu(II) diffusing in the pores of the composites, the diffusion resistance increased, and resulting in the decrease of diffusion rates ($k_{intra,2}$). The final stage was the equilibrium period, during which the intra-particle diffusion rate ($k_{intra,3}$) slowed down and reached to equilibrium. Furthermore, Fig. 8d, revealed that the line dose not passes through the origin, expressing that film diffusion and intra-particle diffusion involved in the adsorption process.[53]

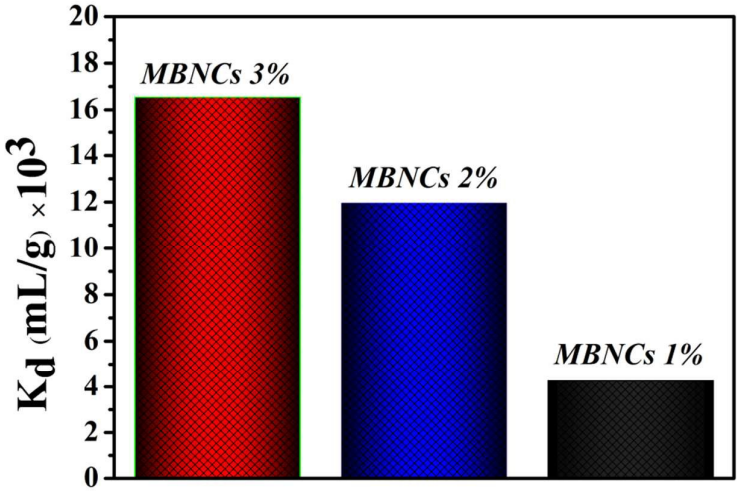

Fig. 9. Distribution coefficients for tree types of MBNCs.

Table 2. Adsorption quality and distribution coefficient parameters for Cu(II) solution (10 mg L^{-1}, pH=4.0) on three types of MBNCs.

sample	Cu(II) content solution ($mg\ L^{-1}$)		Cu(II) Removal efficiency (%)	Cu(II) Adsorbed on sorbent		$K_d\ (mL\ g^{-1})$
	Initial (C_i)	Final (C_e)		($mg\ g^{-1}$)	($\mu\ mol\ g^{-1}$)	
MBNCs 1%	10	1.90	81.02	8.10	127.47	4.26×10^3
MBNCs 2%	10	0.77	92.24	9.22	145.09	11.97×10^3
MBNCs 3%	10	0.57	94.29	9.43	148.39	16.54×10^3

New Journal of Chemistry Accepted Manuscript

Table 3. Fitting of kinetic models for adsorption of Cu(II) on MBNCs

sorbent	$q_{e,exp}$	Pseudo second order			Elovich		Intra-particle diffusion		
	$(mg\ g^{-1})$	k_{ad} $(g\ mg^{-1}min^{-1})$	$q_{e,cal}$ $(mg\ g^{-1})$	R^2	β $(mg\ g^{-1}min^{-1})$	R^2	k_{intra} $(mg\ g^{-1}min^{-1})$	C	R^2
MBNCs 1%	8.10	6.37×10^{-3}	8.85	0.9986	0.6468	0.9282	0.3222	3.8368	0.8029
MBNCs 2%	9.22	7.57×10^{-3}	9.89	0.9983	0.6311	0.8897	0.3252	4.9782	0.7464
MBNCs 3%	9.43	9.66×10^{-3}	9.96	0.9987	0.7093	0.8677	0.2878	5.6869	0.7200

4. Conclusions

In summary, this work has represented fabricating a modified nano-boehmite/poly(methyl methacrylate) nanocomposites with 1, 2 and 3 wt% by in-situ method with good adsorption capacity for Cu(II) ions in aqueous solution. Experimental data revealed that the addition of nanoboehmite as nanofillers into polymer matrix led to improvement of the thermal properties and increasing the active sites of nanocomposites. Nanocomposites with modified boehmite content of 3% showed excellent affinity for copper, adsorption more than 94% of copper ions in 120 minutes and optimum pH of 4. Also, the three adsorption kinetics including pseudo second order, Elovich and intra-particle diffusion equations were discussed briefly to understand the adsorption procedure. The adsorption kinetics analysis of Cu(II) was found to have the best fit to the pseudo second order model with the R^2 of 0.99. Also, intra-particle diffusion was involved in the adsorption process. Therefore, these nanocomposites could be considered as a good adsorbent for removal copper from aqueous solutions.

Acknowledgments

This work was partially funded by the Research Affairs Division of Isfahan University of Technology (IUT)and Iran Nanotechnology Initiative Council (INIC).

New Journal of Chemistry Accepted Manuscript

References

1. P. M. Ajayan, L. S. Schadler and P. V. Braun, *Nanocomposite science and technology*, John Wiley & Sons, 2006.
2. G. Q. Lu, X. S. Zhao and T. K. Wei, *Nanoporous materials: science and engineering*, Imperial College Press, 2004.
3. C. Sanchez, B. Julian, P. Belleville and M. Popall, *Journal of Materials Chemistry*, 2005, **15**, 3559-3592.
4. J. Liu, S. Z. Qiao and Q. H. Hu, *Small*, 2011, **7**, 425-443.
5. G. Mohammadnezhad, M. Dinari, R. Soltani and Z. Bozorgmehr, *Applied Surface Science*, 2015, **346**, 182-188.
6. C.-W. Lee, S.-B. Yoon, H.-K. Kim, H.-C. Youn, J. Han, K. C. Roh and K.-B. Kim, *Journal of Materials Chemistry A*, 2015, **3**, 2314-2322.
7. M. Dinari, G. Mohammadnezhad and A. Nabiyan, *Colloid and Polymer Science,* 2015*,* **293**, 1569-1575.
8. S. Mallakpour, M. Dinari and G. Mohammadnezhad, *Progress in Organic Coatings*, 2015, **78**, 300-306.
9. M. Dinari, G. Mohammadnezhad and A. Nabiyan, *Journal of Applied Polymer Science*, 2016, **133**, 43098-43106.
10. S. Brühne, S. Gottlieb, W. Assmus, E. Alig and M. U. Schmidt, *Crystal Growth and Design*, 2008, **8**, 489-493.
11. Q. Yuan, A.-X. Yin, C. Luo, L.-D. Sun, Y.-W. Zhang, W.-T. Duan, H.-C. Liu and C.-H. Yan, *Journal of the American Chemical Society*, 2008, **130**, 3465-3472.
12. H. Huang, L. Wang, Y. Cai, C. Zhou, Y. Yuan, X. Zhang, H. Wan and G. Guan, *CrystEngComm*, 2015, **17**, 1318-1325.
13. Z. Wu, Q. Zhuo, T. Sun and Z. Wang, *Journal of Applied Polymer Science*, 2015, **132**.
14. Y. Zhao, R. L. Frost, W. N. Martens and H. Y. Zhu, *Langmuir*, 2007, **23**, 9850-9859.
15. X. Y. Chen, H. S. Huh and S. W. Lee, *Nanotechnology*, 2007, **18**, 285608.
16. D. Kuang, Y. Fang, H. Liu, C. Frommen and D. Fenske, *Journal of Materials Chemistry*, 2003, **13**, 660-662.
17. A. Dandapat and G. De, *Journal of Materials Chemistry*, 2010, **20**, 3890-3894.
18. D. Jana, A. Dandapat and G. De, *Langmuir*, 2010, **26**, 12177-12184.
19. N. M. Vitorino, A. V. Kovalevsky, J. C. Abrantes and J. Frade, *Journal of the European Ceramic Society*, 2015, **35**, 3119-3125.
20. J. Zhang, Q. Ji, P. Zhang, Y. Xia and Q. Kong, *Polymer Degradation and Stability*, 2010, **95**, 1211-1218.
21. Y.-X. Zhang, X.-Y. Yu, Z. Jin, Y. Jia, W.-H. Xu, T. Luo, B.-J. Zhu, J.-H. Liu and X.-J. Huang, *Journal of Materials Chemistry*, 2011, **21**, 16550-16557.
22. P. Li, S. Zheng, P. Qing, Y. Chen, L. Tian, X. Zheng and Y. Zhang, *Green Chemistry*, 2014, **16**, 4214-4222.
23. M. Zhang and B. Gao, *Chemical Engineering Journal*, 2013, **226**, 286-292.
24. Y. Zhu, Z. Jiang, L. Zhang, J. Shi and D. Yang, *Industrial & Engineering Chemistry Research*, 2011, **51**, 255-261.
25. N. Nagai, Y.-h. Suzuki, C. Sekikawa, T. Y. Nara, Y. Hakuta, T. Tsunoda and F. Mizukami, *Journal of Materials Chemistry*, 2012, **22**, 3234-3241.
26. A. Laachachi, M. Ferriol, M. Cochez, J.-M. L. Cuesta and D. Ruch, *Polymer Degradation and Stability*, 2009, **94**, 1373-1378.
27. M. Monti and G. Camino, *Polymer Degradation and Stability*, 2013, **98**, 1838-1846.
28. X. Huang and W. J. Brittain, *Macromolecules*, 2001, **34**, 3255-3260.
29. V. Mittal, *In-situ synthesis of polymer nanocomposites*, John Wiley & Sons, 2011.
30. M. Ikegame, K. Tajima and T. Aida, *Angewandte Chemie International Edition*, 2003, **42**, 2154-2157.
31. M. Erceg, D. Jozić, I. Banovac, S. Perinović and S. Bernstorff, *Thermochimica acta*, 2014, **579**, 86-92.

New Journal of Chemistry Accepted Manuscript

32. K. Maeda, R. Takamatsu, M. Mochizuki, K. Kawawa and A. Kondo, *Dalton transactions*, 2013, **42**, 10424-10432.
33. V. K. Tomer and S. Duhan, *Sensors and Actuators B: Chemical*, 2015, **212**, 517-525.
34. L. Wei, N. Hu and Y. Zhang, *Materials*, 2010, **3**, 4066-4079.
35. M. Dinari, G. Mohammadnezhad and R. Soltani, *RSC Advances,* 2016 in press DOI: 10.1039/C5RA23500F.
36. S. Hashemian, H. Saffari and S. Ragabion, *Water, Air, & Soil Pollution*, 2015, **226**, 1-10.
37. P. Kanagaraj, A. Nagendran, D. Rana, T. Matsuura, S. Neelakandan, T. Karthikkumar and A. Muthumeenal, *Applied Surface Science*, 2015, **329**, 165-173.
38. H. Simsek, M. Kobya, E. Khan and A. N. Bezbaruah, *Environmental technology*, 2015, **36**, 1612-1622.
39. M. R. Awual, G. E. Eldesoky, T. Yaita, M. Naushad, H. Shiwaku, Z. A. AlOthman and S. Suzuki, *Chemical Engineering Journal*, 2015.
40. Y. Zhou, S. Boudesocque, A. Mohamadou and L. Dupont, *Separation Science and Technology*, 2015, **50**, 38-44.
41. K. A. Vo, X. J. Xu, T. G. Li, R. H. Peng, S. L. Liu and X. L. Yue, *Desalination and Water Treatment*, 2015, 1-10.
42. S.-M. Kim, Y.-J. Lee, K.-W. Jun, J.-Y. Park and H. Potdar, *Materials Chemistry and Physics*, 2007, **104**, 56-61.
43. F.-A. Zhang, D.-K. Lee and T. J. Pinnavaia, *Polymer*, 2009, **50**, 4768-4774.
44. Y. S. Lipatov, V. Rosovitskii and V. Babich, *Polymer Mechanics*, 1975, **11**, 933-936.
45. N. G. Turan, S. Elevli and B. Mesci, *Applied Clay Science*, 2011, **52**, 392-399.
46. P. Wang, M. Du, H. Zhu, S. Bao, T. Yang and M. Zou, *Journal of Hazardous Materials*, 2015, **286**, 533-544.
47. W. Yantasee, C. L. Warner, T. Sangvanich, R. S. Addleman, T. G. Carter, R. J. Wiacek, G. E. Fryxell, C. Timchalk and M. G. Warner, *Environmental Science & Technology*, 2007, **41**, 5114-5119.
48. Y. Ho, D. J. Wase and C. Forster, *Environmental Technology*, 1996, **17**, 71-77.
49. Y.-S. Ho, *Journal of hazardous materials*, 2006, **136**, 681-689.
50. C. Namasivayam and K. Ranganathan, *Water Research*, 1995, **29**, 1737-1744.
51. T. A. Saleh, *Desalination and Water Treatment*, 2015, 1-15.
52. S. Wang, K. Wang, C. Dai, H. Shi and J. Li, *Chemical Engineering Journal*, 2015, **262**, 897-903.
53. M. Barakat and R. Kumar, *Journal of Industrial and Engineering Chemistry*, 2015, **23**, 93-99.

New Journal of Chemistry Accepted Manuscript

The addition of nanoboehmite as nanofillers into polymer matrix led to improvement of the thermal properties and increasing the active sites of nanocomposites for Cu(II) removal.

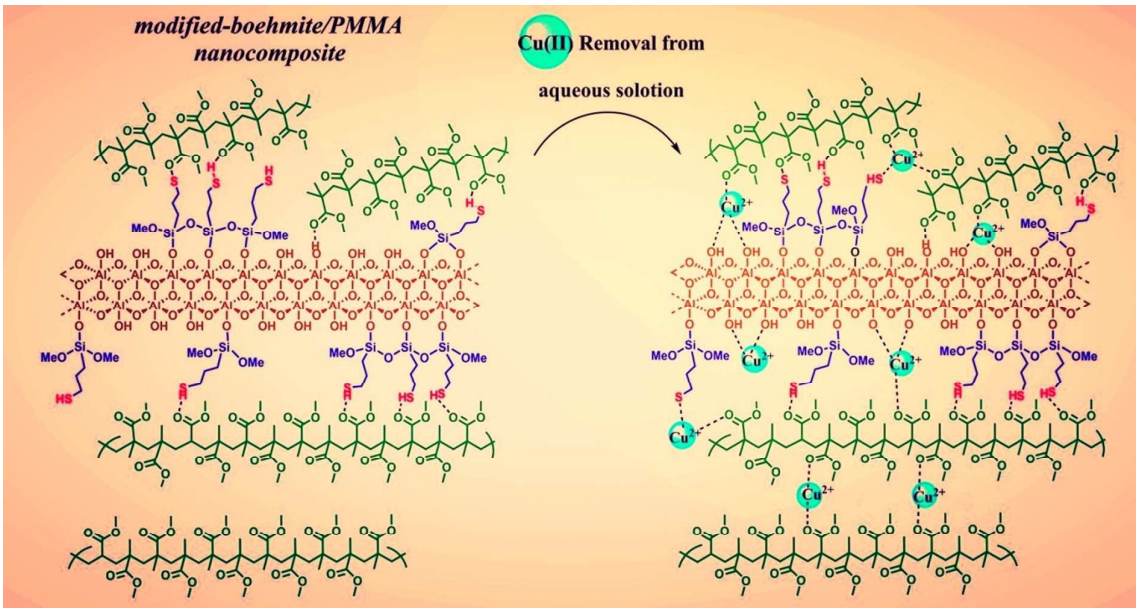

New Journal of Chemistry Accepted Manuscript